ORNL/TM--9005

DE84 007599

ORNL/TM-9005
Dist. Category UC-41

Engineering Physics and Mathematics Division

INTEGRAL MEASUREMENTS OF NEUTRON AND GAMMA-RAY LEAKAGE FLUXES FROM THE LITTLE BOY REPLICA

F. J. Muckenthaler

Work Performed By:

F. J. Muckenthaler
M. B. Diaz*
A. E. Evans*
H. M. Forehand*
G. E. Hansen*
R. E. Malenfant*
R. A. Pederson*
B. Pena*
E. A. Plassmann*
T. F. Wimett*

Manuscript Completed - February 1, 1984
Date Published - March 1984

*Los Alamos National Laboratory, Los Alamos, New Mexico.

OAK RIDGE NATIONAL LABORATORY
Oak Ridge, Tennessee 37830
operated by
UNION CARBIDE CORPORATION
Under Contract No. W-7405-eng-26
for the
Office of Health and Environmental Research
U.S. DEPARTMENT OF ENERGY

TABLE OF CONTENTS

INTEGRAL MEASUREMENTS OF NEUTRON AND GAMMA-RAY LEAKAGE FLUXES FROM THE LITTLE BOY REPLICA

F. J. Muckenthaler

ABSTRACT

This report presents integral measurements of neutron and gamma-ray leakage fluxes from a critical mockup of the Hiroshima bomb Little Boy at Los Alamos National Laboratory with detector systems developed by Oak Ridge National Laboratory. Bonner ball detectors were used to map the neutron fluxes in the horizontal midplane at various distances from the mockup and for selected polar angles, keeping the source-detector separation constant. Gamma-ray energy deposition measurements were made with thermoluminescent detectors at several locations on the iron shell of the source mockup. The measurements were performed as part of a larger program to provide benchmark data for testing the methods used to calculate the radiation released from the Little Boy bomb over Hiroshima.

1. INTRODUCTION

A program initiated by the National Academy of Sciences of the United States is currently under way to reassess the doses that were received by those exposed to radiation from the atomic bomb explosions over the Japanese cities of Hiroshima and Nagasaki during World War II. As part of this program, measurements have been made of the neutron and gamma-ray leakage spectra and dose rates from a controlled-source replica (mockup) of the Hiroshima gun bomb (Little Boy). The mockup was assembled in the Critical Assembly Facility (Kiva #2) at Los Alamos National Laboratory (LANL) and consisted of an outer iron shell fitted with internal fissile parts such that sustained operation of the device could be maintained. The measurements of radiation leakage from this device were made by teams from several laboratories in the United States and Canada in order to develop benchmark data for testing the methods used to calculate the radiation emitted from the Hiroshima bomb.

This report describes a set of measurements made on the Little Boy mockup using detector systems developed by the Engineering Physics Division of Oak Ridge National Laboratory (ORNL). Measurements of the neutron leakage flux were made with Bonner ball detectors at various distances from the mockup and gamma-ray energy deposition measurements were made with thermoluminescent detectors at various locations on the iron shell. It is anticipated that an analysis of the measurements with the computational methods of interest will also be performed at ORNL.

2. EXPERIMENTAL CONFIGURATION

The mockup of the Hiroshima bomb (Little Boy) was located approximately in the center of the LANL Critical Assembly Facility, as shown in Fig. 1. Two other critical assembly devices were also in the building during the measurements: one to the south of Little Boy (called Flattop) and the other to the north (called Big Ten). Both devices used uranium as reflectors, but neither was made active during our measurements.

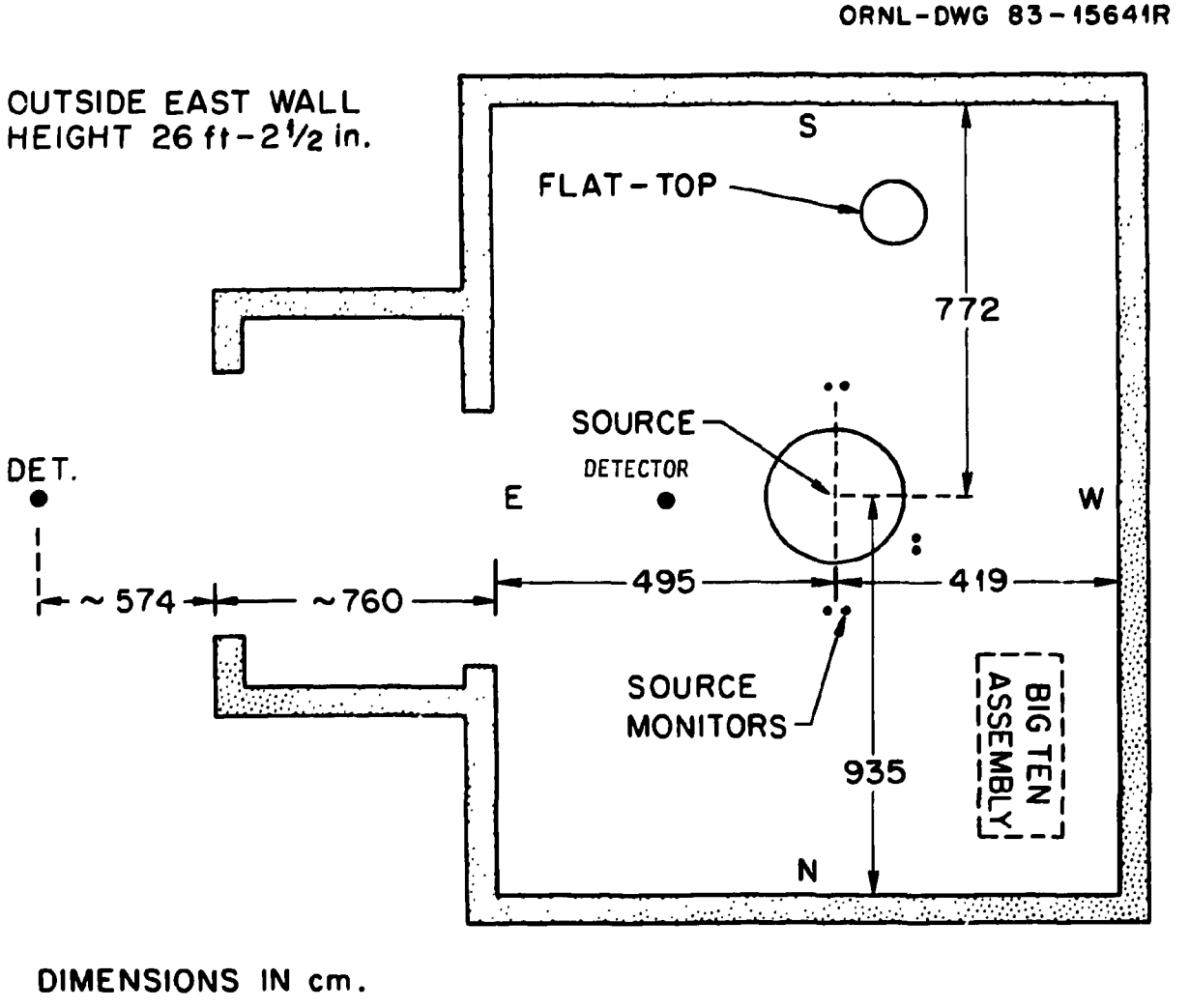

Fig. 1. Physical dimensions inside Kiva #2 at Pajarito Canyon site.

The engineering features of the Little Boy mockup are classified and thus cannot be described here. As noted above, the mockup was housed in an iron shell. The nose of the shell was pointed vertically upward, as shown in Figs. 2 and 3. The center of the source was 31.4 cm above the support stand and 231 cm above the floor. The cylindrical portion of the iron shell surrounding the source was 71 cm in diameter. The overall height of the shell was 91.2 cm (including the hemispheric enclosure atop the mockup but not the 1.91-cm-diameter bolt which protruded 4.90 cm above the center of the dome).

A line due east from the center of the mockup source was selected as the reference for all the detector traverses. This direction allowed the measurements to be extended beyond the building interior, since the detectors could pass through a large opening in the wall that served as a vehicle entry into the building (see Fig. 1). Movement in this direction not only helped to minimize the wall-scattered contribution to the detectors but also provided minimal interference to the detectors serving as monitors of the source intensity.

Shortly after the experiment was begun a traversing mechanism (made of aluminum) was added to the experimental configuration, which greatly facilitated the positioning of the Bonner balls. The mechanism was attached to the iron shell of the mockup using a thick aluminum band, and the mechanism's line of travel was directed eastward as shown in Fig. 2. The mechanism permitted measurements to be made both within the horizontal midplane of the source (from a position close to the iron shell to a distance of 300 cm from the source) and within the vertical midplane of the source (from a position in the horizontal midplane to a point directly above the source). The presence of the aluminum band around the iron shell had a small but significant attenuating effect on the neutrons reaching the source monitors. This decrease in count rate amounted to about 5 percent and this correction to the power level was made throughout the remainder of the experiment.

Background measurements in the horizontal midplane were made with a 62-cm-square by 80-cm-high stack of plain polyethylene placed between the detector and the iron shell as a shadow shield. This shield, which was supported by an overhead crane and was positioned at several locations, is visible in Fig. 3.

3. INSTRUMENTATION

3.1 SOURCE MONITORS

The fission rate from the source was monitored during each run by four detectors: three BF_3 counters covered with polyethylene or cadmium and an ion chamber whose output from a "linear amplifier" was recorded on a Brown chart. Data from the chart were averaged for each run and that value, along with data from at least one of the other three detectors, were used to determine the source intensity. Their differences in sensitivity permitted coverage of a wide range of source intensities. Two of the monitors are visible in Fig. 3 as approximately 30-cm-long cylinders alongside the iron shell.

3.2 BONNER BALL DETECTORS

A set of seven Bonner ball detectors were used in this experiment, each measuring an integral of the neutron energy flux weighted by the energy-dependent response function for that ball. The detection device of a Bonner ball consists of a 5.1-cm spherical BF_3 detector filled to a pressure of 0.5 atmospheres with a relative $^{10}B/B$ concentration of 0.96. This proportional counter, shown in Fig. 4, is used bare, cadmium covered, or enclosed in various thicknesses of polyethylene shells surrounded by cadmium. (In these measurements, the polyethylene diameters were 3, 5, 8, 10, and 12 in.) Bonner ball experimental results are predicted analytically by folding a calculated neutron spectrum with the Bonner ball response functions calculated by Maerker et al.[1] and C. E. Burgart et al.[2]

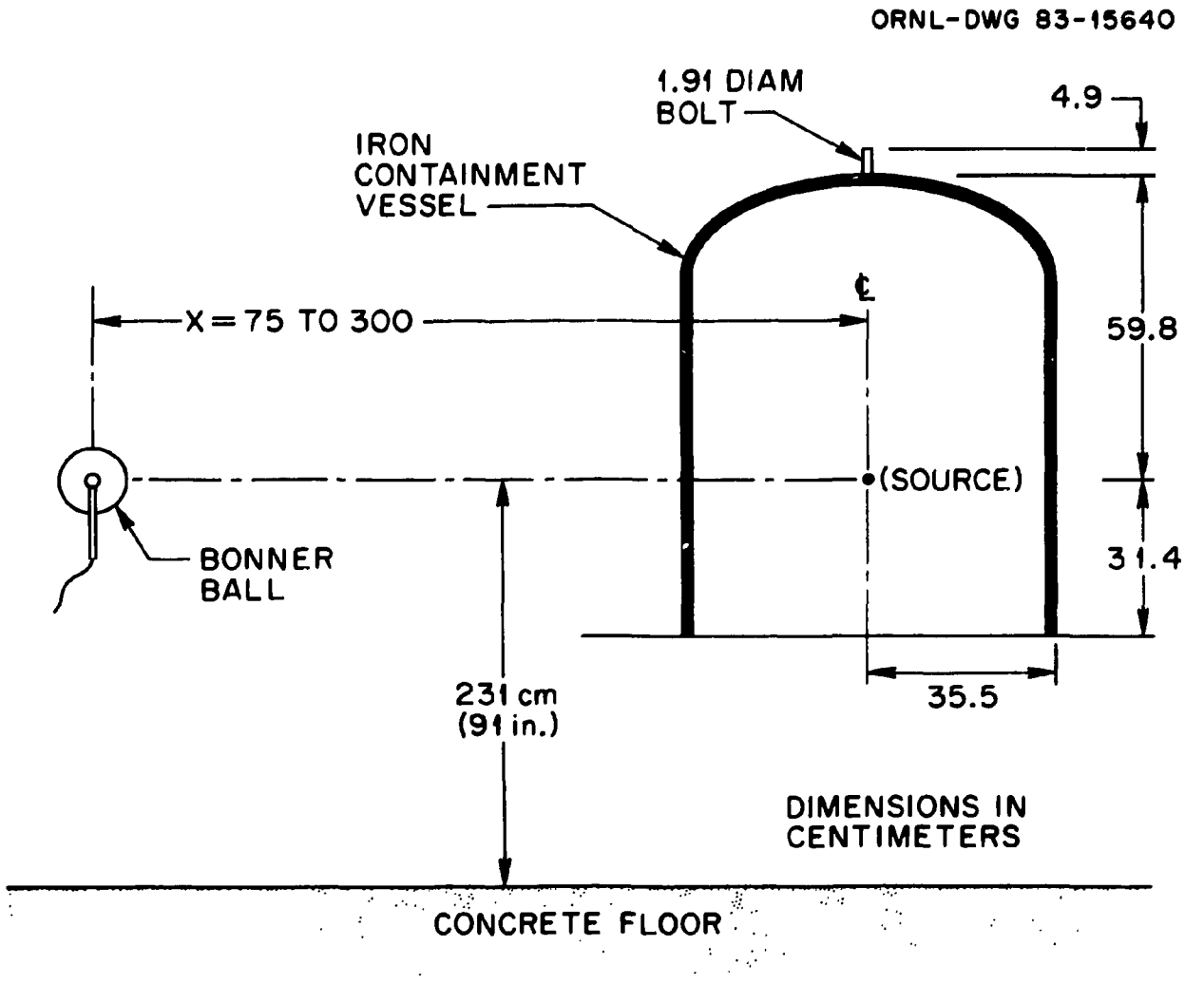

Fig. 2. Plan view of source-detector mockup.

ORNL/PHOTO-4164-83

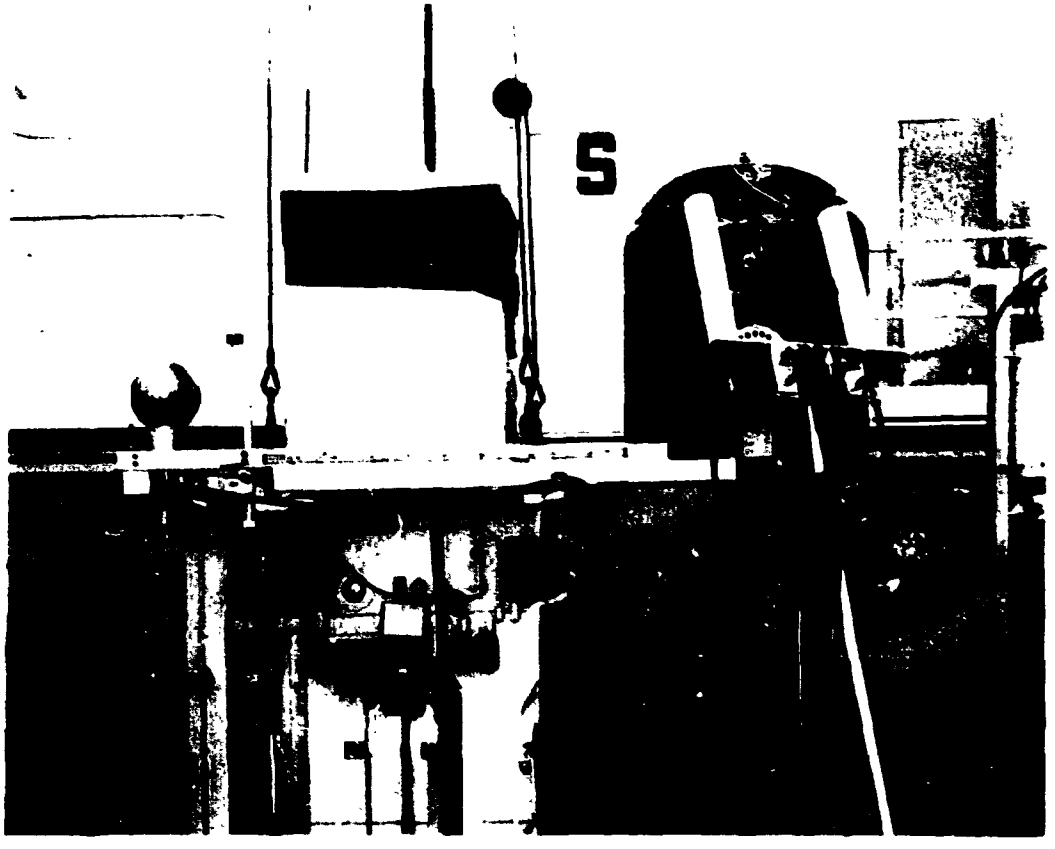

Fig. 3. Experimental configuration showing detector, shadow shield, source and source monitors inside Kiva #2.

ORNL/PHOTO-0486-74A

Fig. 4. Photograph of the 3-, 6-, and 10-in. Bonner balls.

3.3 THERMOLUMINESCENT DETECTORS

The thermoluminescent detectors (TLDs) used for the gamma-ray energy deposition measurements consisted of CaF_2:Mn chips purchased from the Harshaw Chemical Company. They were 0.3175 cm on a side and approximately 0.089 cm thick. The chips were enclosed in iron capsules both during their calibration and during the measurements. The iron capsule was designed to provide a thickness greater than the maximum path length of the electrons induced from the incident gamma ray. The response of the chips was calibrated by exposing them to a known dose rate using a ^{60}Co gamma-ray source. Proper calibration of the TLDs relates the energy deposition to the intensity of the radiation field at each TLD location.

4. MEASUREMENTS

4.1 NEUTRON FLUX MEASUREMENTS

The data plan called for two series of Bonner ball measurements: one to map the flux in the horizontal midplane of the mockup source as a function of distance from the source, and the other to map the flux in the vertical midplane while keeping the source-detector separation distance constant (see Table 1a). Top priority was assigned to the measurements in the horizontal midplane, with the detector traverses extending along the horizontal axis out to 300 cm from the source center. The closest point considered was 75 cm, with intermediate locations at 150, 200, and 250 cm. At each location beyond 75 cm, measurements with the 5-, 8-, 10-, and 12-in. Bonner balls were made with and without the shadow shield between the source and detector. At 150 cm it was feasible to make only one background measurement; with the detectors at 200 cm and beyond it was possible to make measurements for two or more shadow shield positions. This procedure allowed a determination of the contribution to the measured flux by air- and structure-scattered neutrons and thus permitted the background levels to be more closely defined. (Note: The shadow shield also affected the counting rates of the source monitors, and the power levels were corrected accordingly.)

A complete series of Bonner ball measurements were made at the 75-cm location; that is, measurements were made with the bare and cadmium-covered balls and also with the 3-, 5-, 8-, 10-, and 12-in.-diameter balls. For measurements beyond that point, only the 5-, 8-, 10-, and 12-in.-diameter balls were used. The output from one or more of the source monitors was used to normalize each detector measurement to the source strength, thus allowing the count rate to be quoted on a per fission basis. The results are given in Table 2.

Following the measurements along the horizontal traverse, measurements were made outside the building at a distance of 1829 cm from the source centerline. At this location, the large entryway shown in Fig. 1 served as a port for transmission of the neutron beam. Again, a complete series of Bonner ball measurements were made, both with and without the shadow shield, which in this case was located 935 cm from the source. These results are also given in Table 2.

The measurements as a function of polar angle (within the vertical midplane of the source) were made with the 3-, 5-, 10-, and 12-in. Bonner balls at an essentially constant source-to-detector separation distance of about 80 cm. These results, along with bare and cadmium-covered detector measurements at 0 deg and a cadmium-covered measurement at 90 deg, are given in Table 3.

Table 1a. Program of Bonner ball measurements in LANL Little Boy mockup experiment

Angle (deg)	Detector Location[b]	Bonner Balls[c] Bare	Cd-Cover	3-in.	5-in.	8-in.	10-in.	12-in.	Priority
Azimuthal[a]									
0	75 cm	X	X	X	X	X	X	X	1
0	150 cm				X Z	X Z	X Z	X Z	1
0	200 cm				X Z	X Z	X Z	X Z	1
0	250 cm				X Z	X Z	X Z	X Z	1
0	300 cm				X Z	X Z	X Z	X Z	1
0	50 ft	X	X	X	X	X	X	X	3
Polar[d]									
0	75 cm	X	X	X	X		X	X	2
15	75 cm			X	X		X		2
30	75 cm			X	X		X		2
45	75 cm			X	X		X		2
60	75 cm			X	X		X		2
75	75 cm			X	X		X		2

[a]Azimuthal angle reference is east radial.

[b]Distance from center of source.

[c]X = measurement without shadow shield; Z = measurement with shadow shield.

[d]Polar angle reference is vertical centerline of source.

Table 1b. Program of TLD measurements in LANL Little Boy mockup experiment

Angle (deg)	TLDs At power	At zero power	Priority
Azimuthal[a]			
0	X	X	4
45	X	X	4
315	X	X	4
Polar[b]			
0	X	X	4
30	X	X	4
45	X	X	4
70	X	X	4

[a]Azimuthal angle reference is east radial.

[b]Polar angle reference is vertical centerline of source.

Table 2. Bonner ball measurements along horizontal traverse
(polar angle = 90 deg, azimuthal angle = 0 deg)

Distance from source (cm)		Bonner ball count rate (fission^{-1})						
Detector[a]	Shadow shield[b]	Bare	Cd-Covered	3-in.	5-in.	8-in.	10-in.	12-in.
72.6		1.07 (-6)[c,d]						
75		2.96 (-6)	7.50 (-7)	3.77 (-6)	2.05 (-5)	1.55 (-5)	7.95 (-6)	3.50 (-6)
150					5.37 (-6)	3.93 (-6)	2.02 (-6)	9.12 (-7)
150					5.45 (-6)			
150	86.6						1.77 (-7)	7.72 (-8)
150	87.6				7.17 (-7)	3.61 (-7)		
200					3.34 (-6)	2.32 (-6)	1.19 (-6)	5.37 (-7)
200	87.6					4.25 (-7)	2.03 (-7)	8.59 (-8)
200	100				7.81 (-7)			
200	137.6				6.89 (-7)	3.47 (-7)	1.64 (-7)	7.07 (-8)
249						1.62 (-6)	8.17 (-7)	3.75 (-7)
249	87.6					4.22 (-7)		8.48 (-8)
249	88.8						1.96 (-7)	
249	125					4.03 (-7)	1.89 (-7)	8.15 (-8)
249	187.6					3.41 (-7)	1.59 (-7)	6.83 (-8)
250					2.38 (-6)			
250	125				7.78 (-7)			
250	131				7.73 (-7)			
250	187				6.65 (-7)			
300					1.82 (-6)	1.25 (-6)	6.09 (-7)	2.66 (-7)
300	87.6				7.34 (-7)			
300	88.6					3.89 (-7)	1.79 (-7)	7.68 (-8)
300	88.6					3.86 (-7)		
300	150				7.58 (-7)	4.00 (-7)	1.84 (-7)	7.92 (-8)
300	237.6				6.48 (-7)	3.27 (-7)	1.53 (-7)	6.67 (-8)
1829		9.04 (-9)	7.17 (-10)	1.24 (-8)	4.47 (-8)	2.93 (-8)	1.43 (-8)	6.32 (-9)
1829	935	8.86 (-9)	6.55 (-10)	8.61 (-9)	2.26 (-8)	1.23 (-8)	5.53 (-9)	2.32 (-9)
1829	935				2.30 (-8)			

[a]Distance from center of detector to center of source.
[b]Distance from center of shadow shield to center of source.
[c]Read: 1.07×10^{-6}.
[d]For this measurement the bare detector was placed inside one half of 12-in. ball cadmium cover, with the open side toward source.

Table 3. Bonner ball measurements within vertical midplane through polar angles from 0 to 90 degrees

Polar angle[a] (deg)	Distance from source[b] (cm)	Bonner ball count rate (fission^{-1})						
		Bare	Cd-Covered	3-in.	5-in.	8-in.	10-in.	12-in.
0	80.1	2.56 (-7)[c]						
0	80.1	5.95 (-8)[d]	4.24 (-8)					
90	80.1		6.82 (-8)					
0	79.6			1.38 (-6)				
15	79.6			1.25 (-6)				
22.5	79.6			1.16 (-6)				
30	79.6			1.18 (-6)				
45	79.6			1.74 (-6)				
60	79.6			2.56 (-6)				
60	79.6			2.54 (-6)				
75	79.6			3.14 (-6)				
90	79.6			3.41 (-6)				
0	79.4				6.39 (-6)			
0	79.4				6.40 (-6)			
15	79.4				5.82 (-6)			
30	79.4				5.48 (-6)			
45	79.4				8.55 (-6)			
60	79.4				1.30 (-5)			
75	79.4				1.65 (-5)			
90	79.4				1.83 (-5)			
-15	79.8						1.97 (-6)	
0	79.8						2.17 (-6)	
15	79.8						1.96 (-6)	
30	79.8						1.96 (-6)	
45	79.8						3.09 (-6)	
60	79.8						5.05 (-6)	
75	79.8						6.40 (-6)	
90	79.8						6.96 (-6)	
0	79.4							9.30 (-7)
30	79.4							8.71 (-7)
60	79.4							2.26 (-6)
90	79.4							3.14 (-6)

[a]Polar angle with respect to vertical axis of source.

[b]Distance from center of detector to center of source.

[c]Read: 2.56×10^{-7}.

[d]For this measurement the bare detector was placed inside one half of 12-in. ball cadmium cover, with the open side toward source.

4.2 GAMMA-RAY FLUX MEASUREMENTS

The data plan for the measurements with the small iron capsules containing four TLDs each is given in Table 1b. Capsules were placed on the periphery of the iron shell of the mockup at several polar and azimuthal angles. Only two runs were made -- one with the assembly maintained near critical and the other with the assembly shut down. Following the measurements, the TLD chips were transported to Oak Ridge National Laboratory where they were read and calibrated. Results from these measurements are given in Table 4.

Table 4. TLD measurements on periphery of iron shell

TLD location[a]		Source intensity	Energy absorbed
Polar Angle (deg)	Azimuthal Angle (deg)	(Fiss·s^{-1})	(MeV·g^{-1}·s^{-1}/fiss·s^{-1})
90	0	1.57 (11)[b]	1.70 (-7) ± 0.08
90	45	1.57 (11)	1.74 (-7) ± 0.08
90	315	1.57 (11)	1.69 (-7) ± 0.07
75	0	1.57 (11)	1.46 (-7) ± 0.07
45	0	1.57 (11)	4.97 (-8) ± 0.42
30	0	1.57 (11)	2.75 (-8) ± 0.142
0	0	1.57 (11)	3.78 (-8) ± 0.39

[a]Polar angle with respect to vertical axis of source; azimuthal angle with respect to east radial through source.
[b]Read: 1.57×10^{11}.

5. DISCUSSION OF RESULTS

5.1 NEUTRON MEASUREMENTS ALONG HORIZONTAL TRAVERSE

The Bonner ball results given in Table 2 for the 75-cm detector location show that the count rates for the 5- and 8-in.-diameter Bonner balls are nearly a factor of six greater than those for the 3- and 12-in.-diameter balls. This indicates low flux values for both low- and high-energy neutrons. Also, the thermal-neutron flux at 75 cm appears to be dominated by room return. This was crudely determined by shielding the bare BF_3 counter with a cadmium layer placed behind the detector, i.e., away from the source. The background-shielded count rate dropped by a factor of three relative to the unshielded count rate.

For the measurements at detector distances beyond 75 cm, it was possible to make direct background measurements. At 150 cm, Table 2 lists only one background value; for each detector position beyond that distance there are two or more values listed. This approach of making more than one

background measurement at each detector location where possible was added to the program when early measurements indicated that an increase in count rate occurred as the shadow shield was moved toward the source. The increase, which was not large but noticeable, was attributed to scattering from the wall on the opposite side from the source. However, the increase was not linear with shadow shield location but tended to level off and then decrease slightly as the shadow shield was moved near the source. This decrease was believed due to the increased solid angle subtended by the shadow shield, with respect to the east wall, thus diminishing the number of neutrons that could scatter back to the detector.

The proper background level for each detector position was determined by plotting the background values as a function of the shadow-shield location with respect to the source and then using a straight line drawn through these points extrapolate back to the source centerline. This centerline value was assumed to be the background level. The measured values, along with these extrapolated values, are plotted in Fig. 5.

The background count rates at the 75-cm detector location were obtained by plotting the extrapolated centerline values obtained from Fig. 5 for each detector as a function of the detector location (150, 200, 250, and 300 cm) and then extrapolating the resulting curves to 75 cm. These curves, along with the foreground and foreground-minus-background curves, are plotted in Figs. 6-9 for the 5-, 8-, 10-, 12-in. Bonner balls respectively.

For the 5-in. Bonner ball at 75 cm, the extrapolated background value is about 7% of the foreground. At the 150-cm location, the background is about 24%, and at 300 cm it is greater than the foreground-background value. The percentage of background is greatest for the 5-in. ball, since its response lies in the energy region between about 1 eV and 2 MeV where most of the high-energy neutrons, having suffered several scatterings, would eventually reside. For the 8-in. ball at 75 cm, the background is about 5%, and for the 10-in. and 12-in. balls, it is about 4%. Whereas the background percentage for the 5-in. ball at 300 cm is 55%, for the 12-in. ball it drops to about 40%. From these results, one can conclude that using the foreground data at 75 cm without a background subtraction would not introduce an error greater than 10%. For detector locations beyond 75 cm, the background must be considered.

5.2 NEUTRON MEASUREMENTS WITHIN VERTICAL MIDPLANE

The results of the Bonner ball traverses as a function of the polar angle presented earlier in Table 3 are also plotted in Fig. 10. The shapes of the curves are similar to the flux distribution predicted for the Little Boy device.[3] The calculations do, however, vary somewhat from the measurements in the region from zero to about 30 deg, where the calculated total flux is basically flat for the first 12 deg, after which there is a sudden rise followed by a gradual tapering off of the flux. The measurements on the Little Boy mockup indicate the count rates drop by about 10-15% when going from 0 to 30 deg before slowly reaching the maximum at 90 deg. This depression in the flux is essentially the same for the detector sensitive to low-energy neutrons (3-in. ball) as for the one sensitive to the high-energy neutrons (12-in. ball). Measurements of the thermal-neutron flux with the bare detector at the polar angle of 0 deg again indicates that the count rate is due primarily to background since partially covering the detector with cadmium, as was done at 90 deg to shield against background, reduced the count rate to about that for the fully cadmium-covered detector.

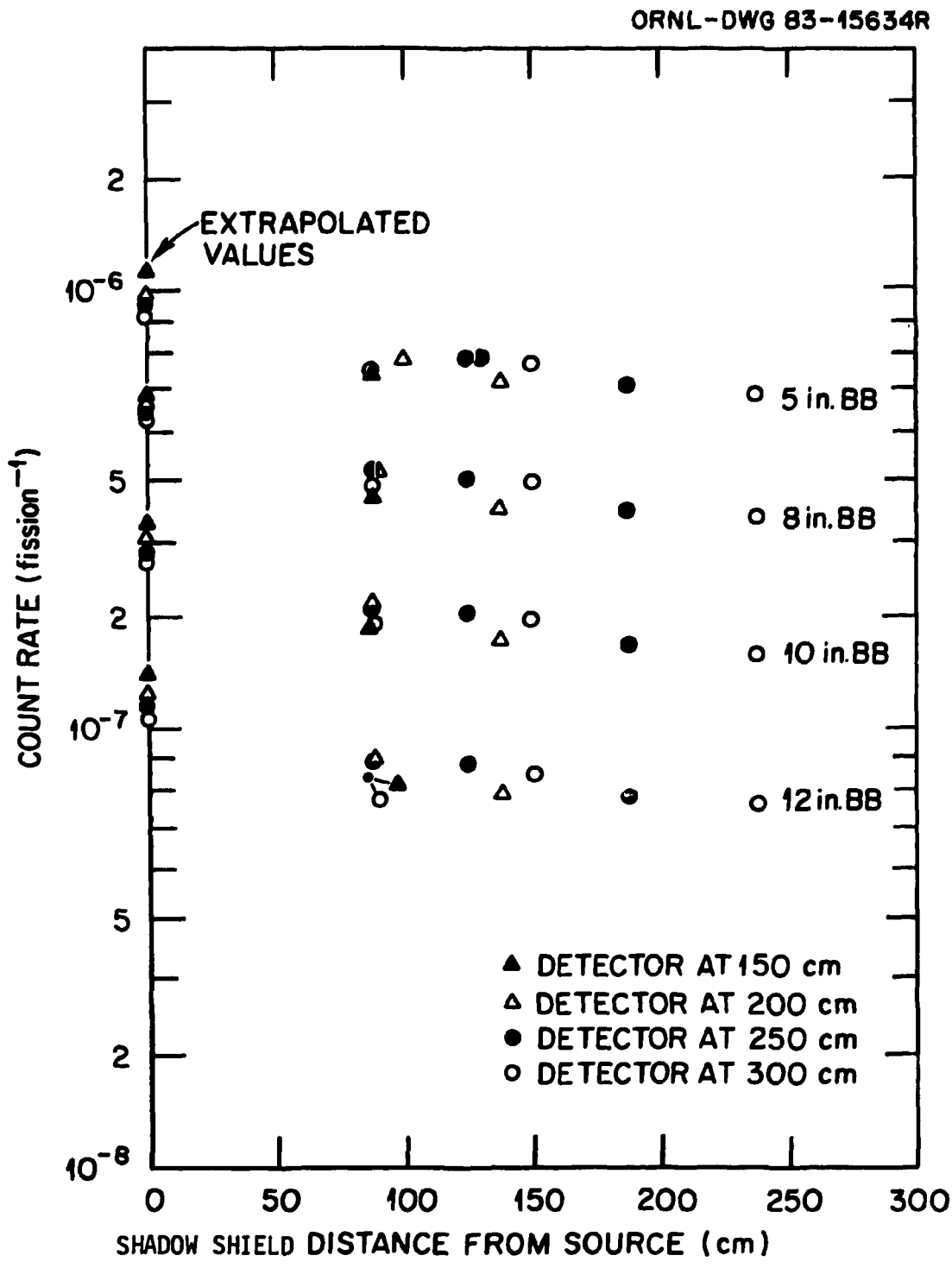

Fig. 5. Bonner ball background count rates at each detector position plotted as a function of shadow shield locations with respect to the source.

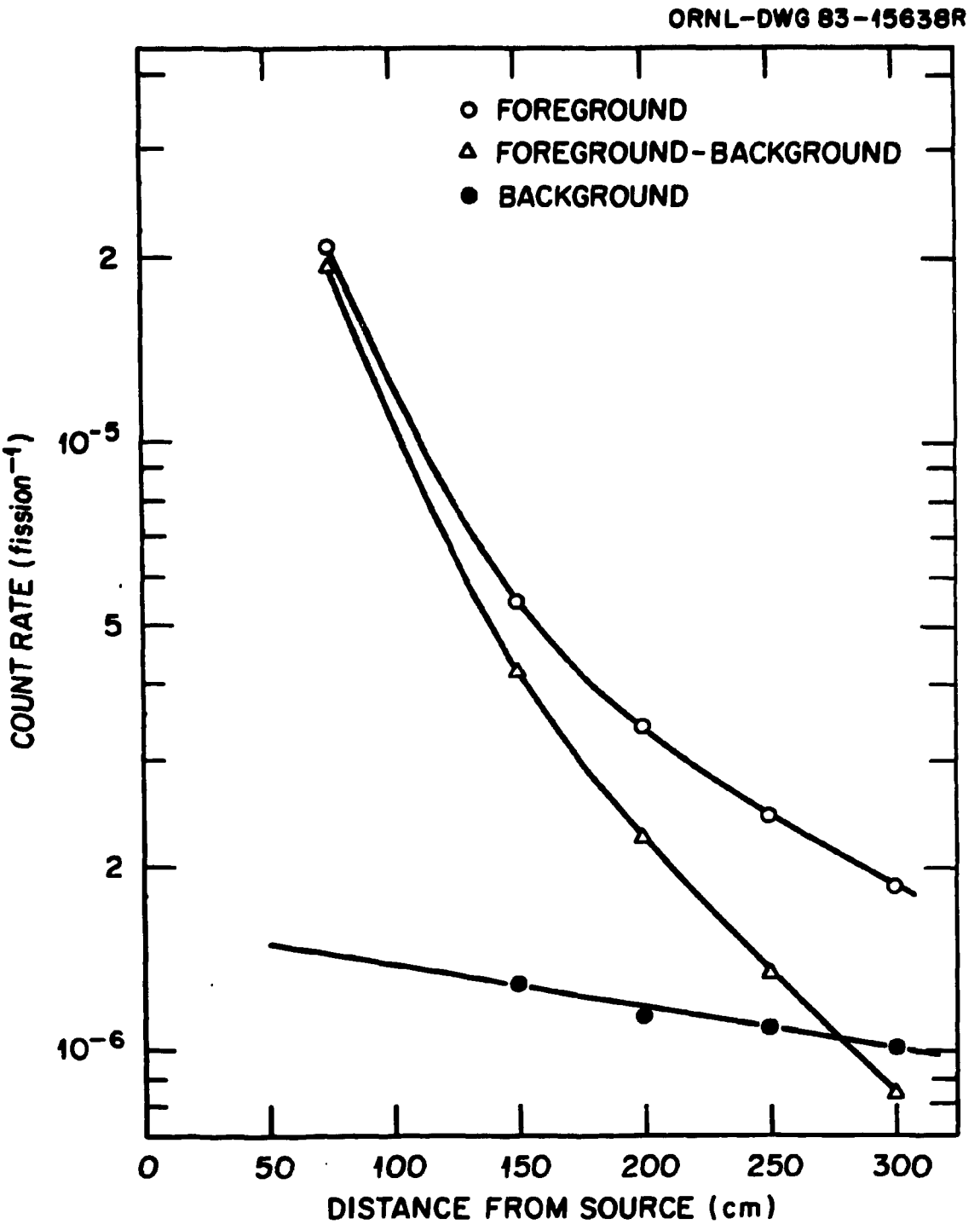

Fig. 6. Plot of foreground, background, and difference measurements with 5-in. Bonner ball along horizontal traverse.

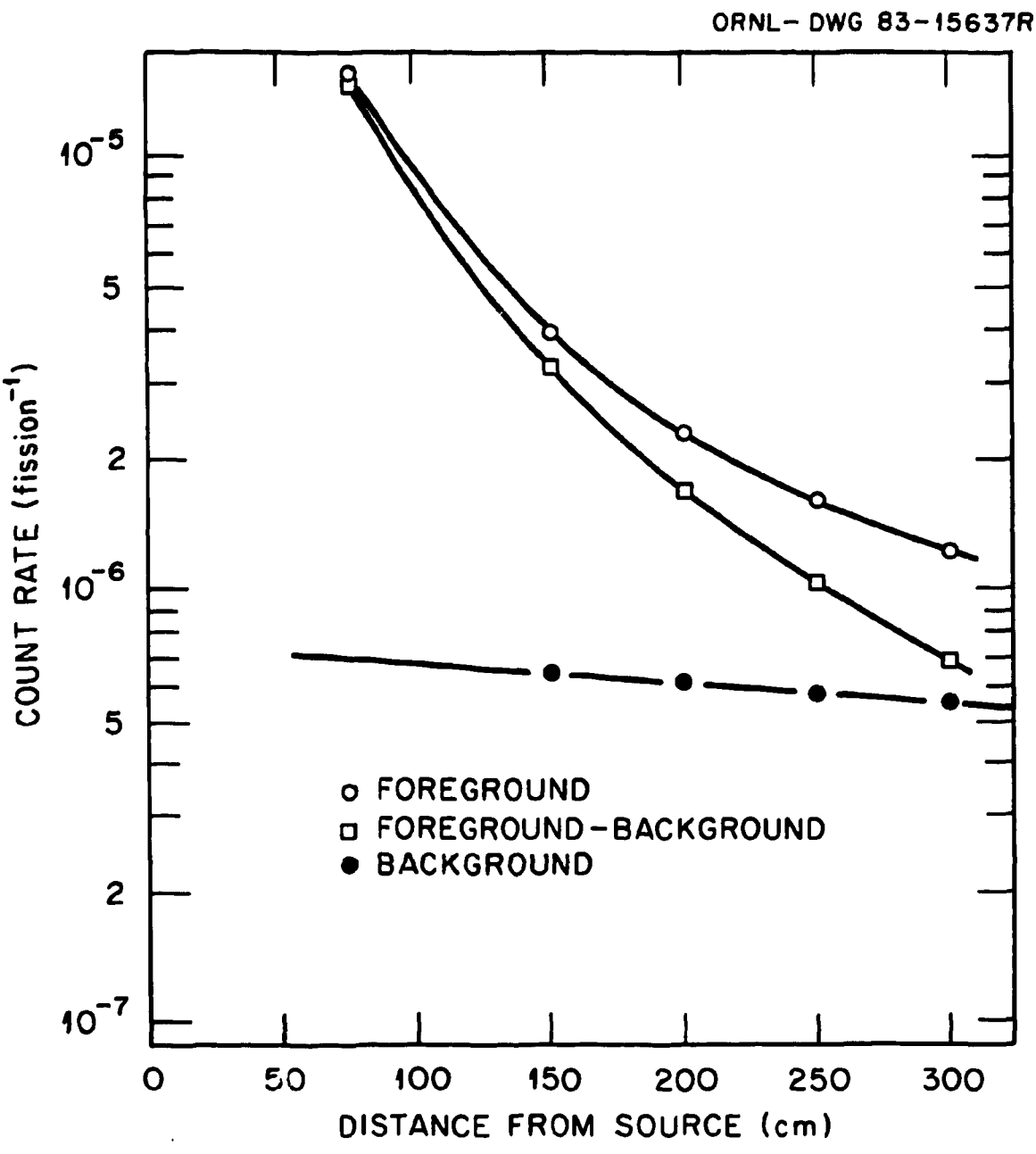

Fig. 7. Plot of foreground, background, and difference measurements with 8-in. Bonner ball along horizontal traverse.

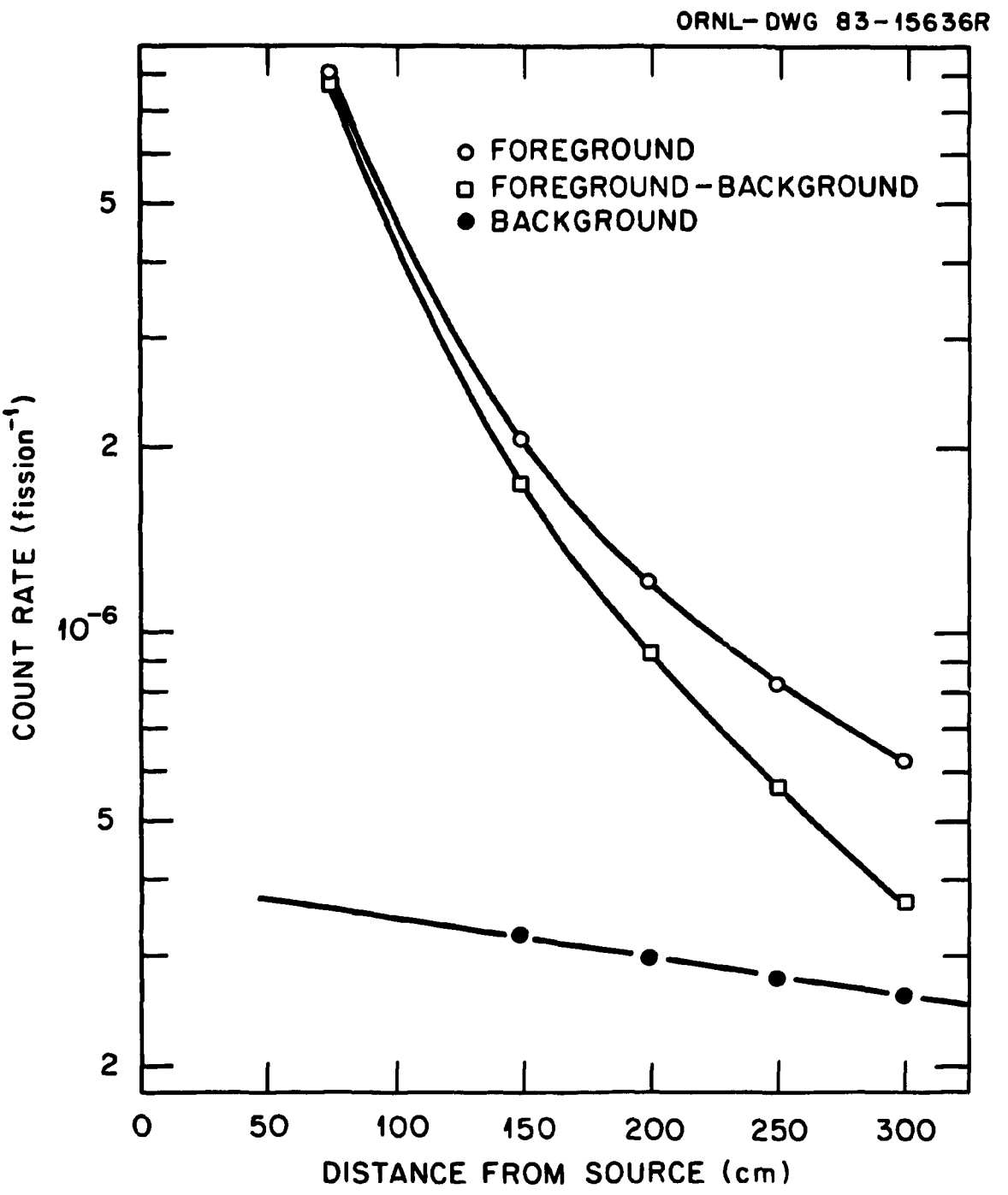

Fig. 8. Plot of foreground, background, and difference measurements with 10-in. Bonner ball along horizontal traverse.

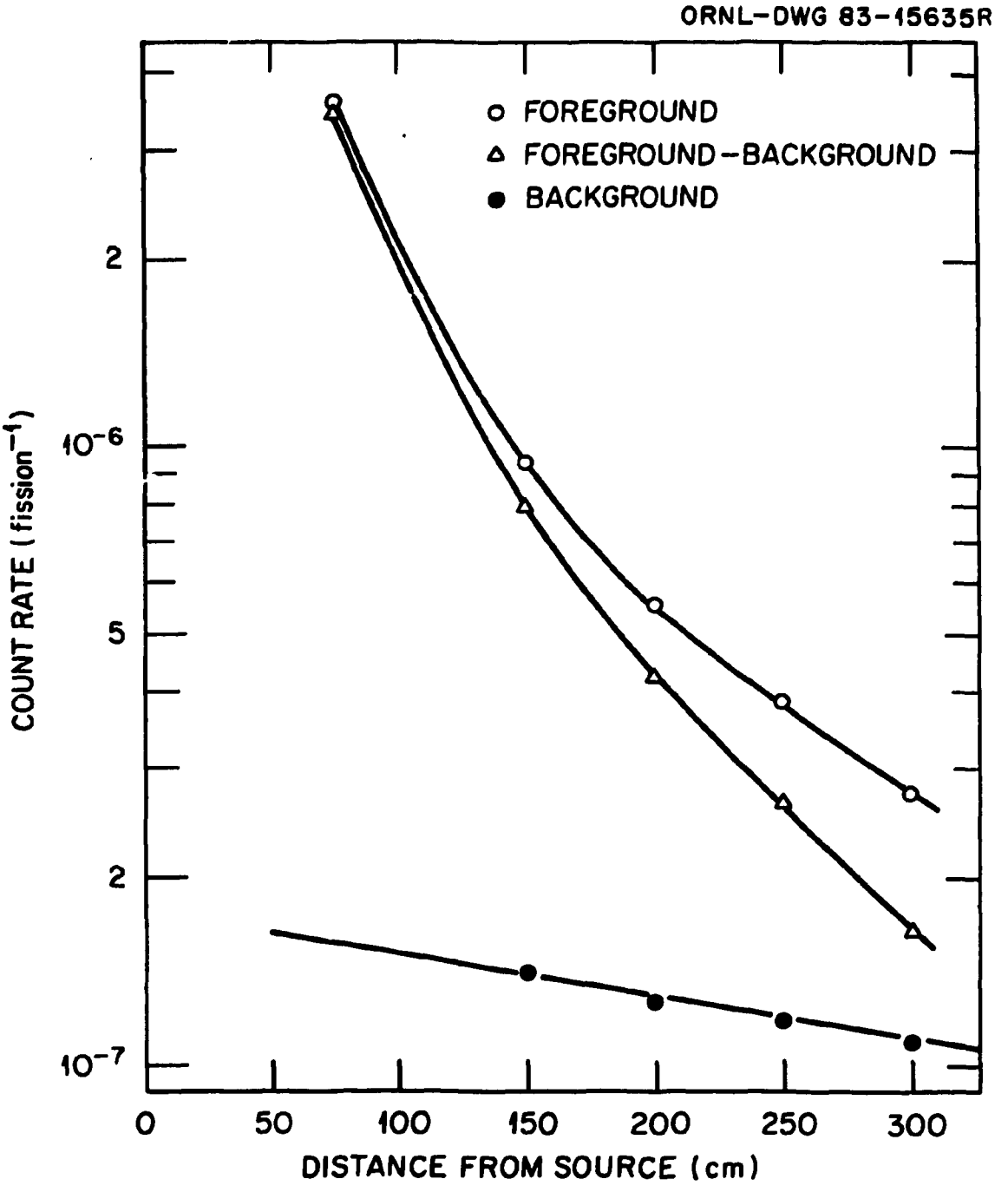

Fig. 9. Plot of foreground, background, and difference measurements with 12-in. Bonner ball along horizontal traverse.

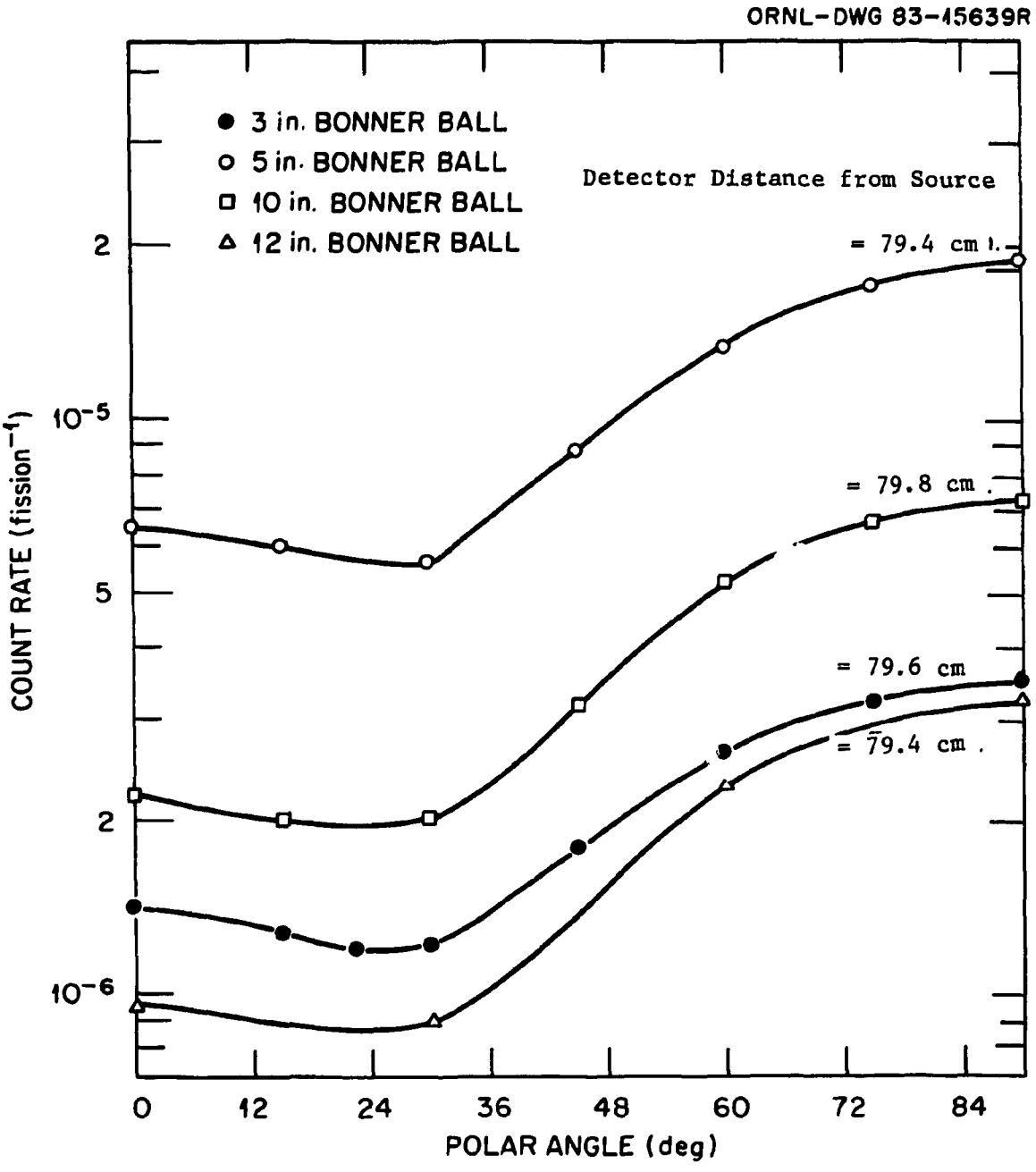

Fig. 10. Plot of Bonner ball measurements as a function of polar angle within vertical midplane.

5.3 GAMMA-RAY MEASUREMENTS ON IRON SHELL

It is to be pointed out that the results given in Table 4 for the TLD measurements have not been normalized for the differences in R^2. Neither have corrections for the neutron interactions in the chips or the spectral $1/f$ factors for the gamma rays from the Little Boy mockup been applied to the data.

6. DISCUSSION OF ERRORS

An intercomparison of the detectors used to monitor the source strength was made since four different detectors were used at various times throughout the experiment. For the cases tested, the variation in power levels between all four detectors was about 5%.

A standard deviation was calculated for a sampling of the Bonner ball count rates and found to be less than 2% for all cases sampled. Calibration of the Bonner ball sensitivity on a daily basis gives about a 5% spread in the range of the count rates over a long period of time. Errors in positioning the detectors should not be more than a few millimeters, which at the 75 cm position would amount to less than a 1% change in count rate. From these values the errors at each data point have been estimated to be less than $\pm 5\%$.

The error quoted is a combination of the standard deviation determined for the mean value obtained from several chip exposures and the error quoted for the Little Boy replica power.

REFERENCES

1. R. E. Maerker, L. R. Williams, F. R. Mynatt, and N. M. Greene, *Response Functions for Bonner Ball Neutron Detectors*, ORNL/TM-3451 (June 18, 1971).
2. C. E. Burgart and M. D. Emmett, *Monte Carlo Calculations of the Response Functions of Bonner Ball Neutron Detectors*, ORNL/TM-3739 (April 3, 1972).
3. P. P. Whalen, Los Alamos National Laboratory, private communication.

ORNL/TM-9005
Dist. Category UC-41

INTERNAL DISTRIBUTION

1-5. L. S. Abbott
6. D. E. Bartine
7. D. G. Cacuci
8. W. W. Engle
9. G. F. Flanagan
10. D. T. Ingersoll
11-15. F. C. Maienschein
16-20. J. J. Manning
21-25. F. J. Muckenthaler
26. R. W. Peelle
27. J. V. Pace
28. L. W. Weston
29. A. Zucker
30. P. W. Dickson, Jr. (Consultant)
31. H. J. C. Kouts (Consultant)
32. D. Steiner (Consultant)
33-34. Central Research Library
35. ORNL Y-12 Technical Library Document Reference Section
36-37. Laboratory Records Department
38. Laboratory Records - RC
39. ORNL Patent Section
40-44. EPD Reports Office

EXTERNAL DISTRIBUTION

45. Office of Assistant Manager for Energy Research and Development, Department of Energy, Oak Ridge Operations Office, Oak Ridge, Tenn. 37831
46-47. DOE Division of Reactor Research and Development, Washington, DC 20545: Director
48. J. A. Auxier, Evaluation Research Corporation, 800 Oak Ridge Turnpike, Oak Ridge, TN 37830
49. David Auton, Nuclear Assessment Directorate, Defense Nuclear Agency, 6801 Telegraph Road, Alexandria, VA 22310
50. Maj. John Campbell, USA, Defense Nuclear Agency, 6801 Telegraph Road, Alexandria, Va. 22310
51. R. F. Christy, Department of Physics, California Institute of Technology, Pasadena, CA 91125
52. C. W. Edington, Associate Director, Office of Health and Environmental Research, ER-70, U.S. Department of Energy (GTN), Washington, DC 20545
53. Charles Eisenhauer, Center for Radiation Research, National Bureau of Standards, Washington, DC 20234
54. W. H. Ellett, Medical Follow-Up Agency, National Research Council, National Academy of Sciences, 2101 Constitution Avenue, NW., Washington, DC 20418
55. D. C. Kaul, Science Applications Incorporated, 1 Woodfield Place Building, Suite 810, 1701 Woodfield Road, Schaumburg, IL 60195

56. W. E. Loewe, D Division, Lawrence Livermore National Laboratory, P. O. Box 808, Livermore, CA 94550
57. Jess Marcum, R & D Associates, Admiralty Way, P. O. Box 9695, Marina del Rey, CA 90291
58. H. A. Robitaille, Defense Research Establishment Ottawa, Department of National Defense, Shirleys Bay, Ottawa, Ontario K1A 0Z4, Canada
59. W. C. Roesch, Consultant, Battelle Pacific Northwest Laboratories, P. O. Box 999, Richland, WA 99352
60. Frederick Seitz, President Emeritus, Rockefeller University, 1230 York Avenue, New York, NY 10021
61. W. K. Sinclair, President, National Council on Radiation Protection and Measurement, 7910 Woodmont Avenue, Suite 1016, Bethesda, MD 20814
62. J. W. Thiessen, Acting Deputy Associate Director, Office of Health and Environmental Research, ER-71, U.S. Department of Energy (GTN), Washington, DC 20545
63. P. P. Whalen, X Division (MS F625), Los Alamos National Laboratory, P. O. Box 1663, Los Alamos, NM 87575
64. W. A. Woolson, Science Applications Incorporated, 1200 Prospect Street, P. O. Box 2351, La Jolla, CA 92038
65. H. O. Wyckoff, Chairman, International Commission on Radiation Units and Measurements, 7910 Woodmont Avenue, Suite 1016, Bethesda, MD 20814
66. R. E. Malenfant, Q2(MS J562), Los Alamos National Laboratory, P. O. Box 1663, Los Alamos, NM 87575

67-301. For distribution as shown in TID-4500 Distribution Category UC-41, Health and Safety